
Adaptive and Interpretable Graph Convolution Networks Using Generalized Pagerank

Kishan Wimalawarne ¹ and Taiji Suzuki ^{1, 2}

¹Department of Mathematical Informatics, Graduate School of Information Science and Technology, The University of Tokyo, Tokyo, Japan

²Center for Advanced Intelligence Project (AIP), RIKEN, Tokyo, Japan

Abstract

We investigate adaptive layer-wise graph convolution in deep GCN models. We propose AdaGPR to learn generalized Pageranks at each layer of a GCNII network to induce adaptive convolution. We show that the generalization bound for AdaGPR is bounded by a polynomial of the eigenvalue spectrum of the normalized adjacency matrix in the order of the number of generalized Pagerank coefficients. By analysing the generalization bounds we show that oversmoothing depends on both the convolutions by the higher orders of the normalized adjacency matrix and the depth of the model. We performed evaluations on node-classification using benchmark real data and show that AdaGPR provides improved accuracies compared to existing graph convolution networks while demonstrating robustness against oversmoothing. Further, we demonstrate that analysis of coefficients of layer-wise generalized Pageranks allows us to qualitatively understand convolution at each layer enabling model interpretations.

1 Introduction

In recent years Graph Convolution Networks (GCN) have gained increased recognition as a versatile tool to learn from graphs. Graph convolution networks use the graph topological structures among the data to extract nonlinear features to perform learning tasks. Many recent advances in graph convolution networks have produced state of the art performances in applications such as social influence prediction [8], relationship modelling [17], recommendation systems [20], and computer vision [22].

Despite the promising capabilities and many novel approaches, GCN still faces several limitations that hinders its full potential in learning with graphs. A well known limitation with GCN is oversmoothing [13], where stacking of multiple convolution layers leads to drop in performance. Oversmoothing is prominent with a model like the Vanila GCN [6], since multiple convolutions by global graph data lead to generalized features that lack the ability learn from labelled data. Recently, many approaches have been proposed to mitigate the effect of oversmoothing. Some of these methods include simple data processing such as data normalization by Pair-Norms [21] and random removal of edges using dropedges [16]. Many other methods use more complex methods such as random walks as employed in ScatterGCN [12] and skipping layers as with JKNet [18]. A notable recent development is GCNII [3], which uses scaled residual layers and addition of the initial layer to each convolution layer. GCNII has reported strong robustness against oversmoothing, however, it often requires a deep network to gain a considerable high accuracy.

Another limitation that we identify with GCN is the lack of adaptability of graph convolution at each layer. Most GCN models apply the same graph convolution method to each layer of a deep network [6, 3]. This not only cause oversmoothing but it may also lead to redundant memory usages and

computations. Furthermore, most GCN models do not provide a systematic approach to understand and interpret graph convolutions applied at each layer of a deep model. In practice, to design a optimal GCN model it is desirable to know the suitable graph convolution method to apply as well as the amount of convolution to be applied at each layer depending on the data and the learning task. Recently proposed GPR-GNN [4] learns a generalized Pagerank within the APPNP model [7] to perform adaptive graph convolution. However, GPR-GNN is a shallow network and does not consider graph convolution in multiple layers, hence, it may not be efficient as a deep GCN model.

In this paper, we investigate adaptive convolution in deep graph convolution networks. In contrast to the widely adapted view of applying the same graph convolution method at each layer, we propose that graph convolution should be different for each layer. In our view, graph convolution should be adaptive in a layer-wise manner where the GCN model should be able to learn how to apply graph convolution depending on the network architecture, nature of the data, and the learning task. We propose AdaGPR to apply adaptive generalized Pageranks at each layer of a GCNII model by learning to predict the coefficients of generalized Pageranks using sparse solvers. By analysing the generalized bounds of AdaGPR, we obtain the Rademacher complexity as a polynomial of the eigenvalue spectrum of the normalized adjacency matrix. Using Rademacher complexity we explain oversmoothing and layer-wise adaptability of the proposed method. We conduct evaluations on node-classification and show that AdaGPR provides better accuracy compared to state of the art GCN methods. As a further advantage of our method, we demonstrate that analysis of the coefficients of layer-wise generalized Pagerank allows us to quantitatively understand layer-wise convolution leading to interpretable GCN models.

2 Review

We start by defining notations used in this paper. Let $G = (V, E)$ a graph with nodes $v_i \in V$, $i = 1, \dots, N$ and edges $(v_i, v_j) \in E$. Let $X \in \mathbb{R}^{N \times p}$ represents a feature matrix with each row representing p features. Let $Y \in \mathbb{R}^{N \times c}$ represents labels of the N nodes with each consisting of c classes. The adjacency matrix of G is represented as $A \in \mathbb{R}^{N \times N}$, and the self-loops added adjacency matrix is $\hat{A} = A + I_N$, where $I_N \in \mathbb{R}^{N \times N}$ is a identity matrix. We denote the diagonal degree matrix of \hat{A} by $\hat{D}_{ij} = \sum_k \hat{A}_{ik} \delta_{ij}$, then the normalized adjacency matrix is $\tilde{A} = \hat{D}^{-1/2} \hat{A} \hat{D}^{-1/2}$.

The most simple graph convolution network (also known as the Vanilla GCN) was proposed in [6], where each layer of a multilayer network is multiplied by the normalized graph adjacency matrix before applying a nonlinear activation function. A 2-layer Vanilla GCN is given as

$$Z = \text{softmax}(\tilde{A} \text{ReLU}(\tilde{A} X W_0) W_1),$$

where $W_0 \in \mathbb{R}^{p \times h}$ and $W_1 \in \mathbb{R}^{h \times c}$ are learning weights with h hidden units. It is well observed that the Vanilla GCN model is highly susceptible to oversmoothing with the increase of depth [13, 3].

Recently, many methods that have been proposed to overcome oversmoothing [21, 16, 3]. Among them, the integration of the highly celebrated web hyperlink modelling method Pagerank [2] as a graph convolution mechanism has gained a considerable attention [7, 4]. It has been established [7] that the use of the self-looped normalized adjacency matrix \tilde{A} as a random walk matrix in Pagerank naturally leads to the personalized Pagerank (PPR) [2]. The personalised Pagerank matrix is given as

$$PPR(\alpha) := (I_N - (1 - \alpha)\tilde{A})^{-1}, \quad (1)$$

where $\alpha \in (0, 1)$ is known as the teleportation parameter specifying the probability that a random walk returns to the original node without traversing to a neighbouring link.

Pagerank based GCN models have been developed [7] by applying a Pagerank on the features of a multilinear neural network that learns on the input data prior to the output layer. It has been argued [7] that the natural ability of the Pagerank to learn from local connectivities in a graph is capable to avoid oversmoothing in GCN models. Formally, the APPNP model proposed in [7] applies a single convolution of a personalized Pagerank to the output of the multilinear network $f_\theta(\cdot)$ parametrized by θ prior to the output as

$$H = f_\theta(X), \quad Z^K = \text{softmax}((I_N - (1 - \alpha)\tilde{A})^{-1} H). \quad (2)$$

To overcome the computational burden of the matrix inversion computation in the personalized Pagerank, the APPNP has been developed [7] the uses the power iteration of the Personalized Pagerank.

Given L power iterations, the APPNP model extends from (2) as

$$\begin{aligned} Z^0 &= H = f_\theta(X), \\ Z^{l+1} &= (1 - \alpha) \tilde{A} Z^l + \alpha H, \quad l = 0, \dots, L - 1, \\ Z &= \text{softmax}((1 - \alpha) \tilde{A} Z^L + \alpha H). \end{aligned} \quad (3)$$

Recently, APPNP has become a useful building block to develop novel GCN models. GCNII [3] proposed to multiply on each convolution step of APPNP using scaled residual weights and nonlinear activations. The resulting $l + 1$ th convolution layer of GCNII is given as

$$H^{(l+1)} = \sigma \left(\left((1 - \alpha_l) \tilde{A} H^{(l)} + \alpha_l H^{(0)} \right) \left((1 - \beta_l) I_N + \beta_l W^{(l)} \right) \right), \quad (4)$$

where $\sigma(\cdot)$ is the ReLU operator, $H_0 = \sigma(XW_0)$ is the output from initial layer, $W^{(0)}$ and $W^{(l)}$ are weight matrices, and $\alpha_l \in [0, 1]$ and $\beta_l \in [0, 1]$ are user-defined parameters.

Another extension of the APPNP is GPR-GNN [4], which substitute a generalized Pagerank in place of the power iterated personalized Pagerank. The generalized Pagerank (GPR) [9] can be viewed as the expansion of (1) with K powers of the normalized adjacency matrix with coefficients $\mu = [\mu_0, \dots, \mu_{K-1}] \in [0, 1]^K$ as

$$GPR(\mu) := \sum_{k=0}^{K-1} \mu_k \tilde{A}^k. \quad (5)$$

The advantage of using GPR is the ability to learn the coefficients μ from the data [9], hence, it is a useful tool to perform adaptive convolution [4]. Formally, the GPR-GNN is expressed as

$$\begin{aligned} P &= \text{softmax}(Z), \quad Z = \sum_{k=0}^{K-1} \mu_k H^{(k)}, \\ H^{(k)} &= \tilde{A} H^{(k-1)}, \quad H_{i:}^{(0)} = f_\theta(X_{i:}), \end{aligned} \quad (6)$$

where θ represents learning parameters of a multilayer network and μ is learned using message passing.

There are several limitations in above models. Both APPNP and GPR-GNN apply only a single convolution by variants of the Pagerank on the learned representation prior to the output layer. Further, these models do not apply any learning weights and nonlinear activations after convolution, hence, they do not create deep GCN models. On the other hand, the GCNII allows us to develop deep models that are robust against the oversmoothing, however, it relies solely on convolutions by the normalized adjacency matrix lacking any adaptive convolution or any benefits offered by the Pagerank.

3 Proposed Method

We propose adaptive layer-wise graph convolution for deep graph conventional models. Our approach is simple, where we propose to apply a generalised Pagerank at each layer of the GCNII and learn coefficients of generalised Pageranks.

As in GCNII, we use a initial layer $H^{(0)} = \sigma(XW^{(0)})$ without any graph convolution using learning weights $W^{(0)} \in \mathbb{R}^{N \times h}$, where h is the number of hidden units. Given L layers of graph convolutions, we replace the convolution by \tilde{A} at layer l of (4) with the generalized Pagerank (5) using K orders of \tilde{A} and coefficients $\mu^{(l)} = (\mu_0^{(l)}, \dots, \mu_{K-1}^{(l)}) \in [0, 1]^K$. Additionally, we impose the constraint $\sum_{k=0}^{K-1} \mu_k^{(l)} = 1$. In order to make generalized Pagerank adaptive for each layer, the model needs to learn coefficients $\mu^{(l)} \in \mathbb{R}^K$, $l = 1, \dots, L$ by using separate learning weights $v^{(l)} \in \mathbb{R}^K$, $l = 1, \dots, L$, respectively. Furthermore, we provide flexibility to apply a suitable activation function $g(\cdot)$ on $v^{(l)}$ in order to obtain specific properties such as sparseness. We call the new graph convolution network AdaGPR, where its $(l + 1)$ th layer is defined as

$$H^{(l+1)} = \sigma \left(\left((1 - \alpha_l) \left(\sum_{k=0}^{K-1} \mu_k^{(l)} \tilde{A}^k \right) H^{(l)} + \alpha_l H^{(0)} \right) \left((1 - \beta_l) I_N + \beta_l W^{(l)} \right) \right), \quad \mu^{(l)} = g(v^{(l)}), \quad (7)$$

where $W^{(l)} \in \mathbb{R}^{h \times h}$, $l = 1, \dots, L-1$ and $W^{(L)} \in \mathbb{R}^{h \times c}$. Similarly to GCNII, parameters α_l and β_l need to be specified by the user or tuned as hyperparameters. As with GCNII [3], we also specify a predefined $\alpha := \alpha_l \in (0, 1)$ for all layers and decaying $\beta_l = \log(\lambda/l + 1) \approx \lambda/l$ where λ is a predefined parameter.

The main advantage with AdaGPR compared to conventional graph convolution methods and GCNII is that it can learn how to apply convolution at each layer. It is obvious that when $\mu_0^{(l)} = 1.0$ or $\mu_1^{(l)} = 1.0$ for all $l = 1, \dots, L$ AdaGPR is equivalent to a multilayer residual network or GCNII, respectively. Again, notice that AdaGPR has a generalized Pagerank at each layer with aggregations and nonlinear activations compared to APPNP and GPR-GNN. To our knowledge AdaGPR is the first graph convolution model to apply layer-wise adaptive Pagerank in a deep graph convolution model.

We point out that AdaGPR has more learning parameters and hyperparameters than GCNII. In practice, we have found that we need to consider K as a hyperparameter that needs to be selected during the training phase. We can also use a different K for each layer, however, that may be impractical due to the large combinations of GPRs we may have to consider. Depending on the learning problem, we may also have to apply a separate weight decay for $v^{(l)}$.

3.1 Learning Sparse Solutions for GPR

There are several ways to learn $\mu^{(l)}$ of (7) such that $\sum_{k=0}^{K-1} \mu_k^{(l)} = 1$. One of the simplest methods is to use the Softmax, however, the resulting $\mu^{(l)}$ may not be sparse which would not give us the desired interpretable results. Variants of Softmax [11] such as sphericalmax and sum-normalization may lead to the same limitation of sparseness in addition to the difficulty of implementing the restriction $\sum_{k=0}^{K-1} \mu_k^{(l)} \neq 0$. Another approach is message passing as used in GPR-GNN [4], however, it can be computationally expensive to implement message passing in a deep GCN model such as our proposed method.

We adopt the recently developed sparse activation function Sparsemax [11] for the task of predicting each $\mu^{(l)}$. Without loss of generality we restate $\mu^{(l)}$ belonging to a $(K-1)$ -dimensional simplex $\Delta^{K-1} := \{\mu^{(l)} \in \mathbb{R}^K | \mathbf{1}^\top \mu^{(l)} = 1, \mu^{(l)} \leq \mathbf{0}\}$, then Sparsemax is the solution of

$$\text{sparsemax}(z^{(l)}) = \underset{\mu^{(l)} \in \Delta^{K-1}}{\operatorname{argmin}} \|\mu^{(l)} - z^{(l)}\|^2. \quad (8)$$

The closed-form solution [11] of (8) is given by $\text{sparsemax}_i(z) = [z_i - \tau(z)]_+$, where $\tau(z) = \frac{(\sum_{j \in k(z)} z_{(j)}) - 1}{k(z)}$ with $k(z) := \max\{k \in [K] | 1 + kz_{(k)} > \sum_{j < k} z_{(j)}\}$ given sorted $z_{(1)} \geq z_{(2)} \geq \dots \geq z_{(K)}$. By empirical evaluations, we found that we can obtain better solutions for AdaGPR by using $\exp(\mu^{(l)})$ instead of $\mu^{(l)}$, which resembles a sparse version of softmax. Our implementations of AdaGPR use the Pytorch code for sparsemax associate with the paper [11]¹.

4 Theoretical Analysis

We analyse generalization bounds for the proposed method to obtain a deeper understanding from a theoretical perspective.

We analyse generalization bounds under transductive settings [5, 14] for semi-supervised node classification. We recall that $X \in \mathbb{R}^{N \times p}$ is the feature matrix of N nodes with an associated graph $G = (V, E)$ and $Y \in \mathbb{R}^{N \times c}$ are the labels of nodes with c classes. Let us consider the sets \mathcal{X} and \mathcal{Y} such that $X \subseteq \mathcal{X}$, $Y \subseteq \mathcal{Y}$ and $(x_i, y_i) \in \mathcal{X} \times \mathcal{Y}$. Let us consider D_{train} and D_{test} as the training and test sets, respectively. Samples are drawn without replacement from D_{train} and D_{test} such that $D_{\text{train}} \cup D_{\text{test}} = V$ and $D_{\text{train}} \cap D_{\text{test}} = \emptyset$. Given $M := |D_{\text{train}}|$ and $U := |D_{\text{test}}|$, we define $Q := 1/M + 1/U$. Let $\mathcal{F} \subset \{\mathcal{X} \rightarrow \mathcal{Y}\}$ be the hypothesis for the transductive learning for AdaGPR. For a predictor $h : \mathcal{X} \rightarrow \mathcal{Y}$, $h \in \mathcal{F}$ and a loss function $l(\cdot, \cdot)$ (e.g. sigmoid, sigmoid cross entropy), we denote the training error by $R(h) = \frac{1}{M} \sum_{n \in V_{\text{train}}} l(h(x_n), y_n)$ and test error by $\hat{R}(h) = \frac{1}{U} \sum_{n \in V_{\text{test}}} l(h(x_n), y_n)$. Using a well-known result from [5], for a given hypothesis class

¹<https://github.com/KrisKorrel/sparsemax-pytorch>

\mathcal{F} we state the generalization bounds based on transductive Rademacher complexity $\mathcal{R}(\mathcal{F}, p)$ with $p \in [0, 0.5]$ and $S := \frac{2(M+U) \min(M, U)}{(2(M+U)-1)(2 \min(M, U)-1)}$ and probability $1 - \delta$ as,

$$R(h) \leq \hat{R}(h) + \mathcal{R}(\mathcal{F}, p) + c_0 Q \sqrt{\min(M, U)} + \sqrt{\frac{SQ}{2} \log \frac{1}{\delta}}, \quad (9)$$

where c_0 is a constant.

For the ease of analysis, we consider unscaled weight in (7) with $\beta_l = 1.0$ and a single $\alpha_l = \alpha \in (0, 1)$ for all layers. We consider a predefined $\mu^{(l)} \in [0, 1]^K$ with $\sum_{k=0}^{K-1} \mu_k^{(l)} = 1$ for each layer l to construct layer-wise a GPR as $\tilde{A}(\mu^{(l)}) := \sum_{k=0}^{K-1} \mu_k^{(l)} \tilde{A}^k$. Let us define $C_0, \dots, C_L \in \mathbb{N}_+$ with $C_0 = p$, $C_1 = \dots = C_{L-1} = h$ and $C_L = c$ to represent the dimensions of hidden layers and the output of AdaGPR. For the semi-supervised learning (transductive setting) we specify $x = X[n, :]$, then we define the hypothesis class for AdaGPR as

$$\mathcal{F} = \left\{ x \rightarrow \sigma \left((1 - \alpha) A(\mu^{(L)}) \sigma \left(\dots ((1 - \alpha) A(\mu^{(1)}) \sigma(XW^{(0)}) + \alpha \sigma(XW^{(0)})) W^{(1)} + \dots + \alpha \sigma(XW^{(0)}) \right) W^{(L)} \right)_n \middle| \|W_c^{(l)}\|_1 \leq B^{(l)} \text{ for all } c \in [C_{l+1}] \right\}, \quad (10)$$

where $W^{(l)} \in \mathbb{R}^{C_l \times C_{l+1}}$ $l = 0, \dots, L$, and $\sigma : \mathbb{R} \rightarrow \mathbb{R}$ is a 1-Lipschitz function such that $\sigma(0) = 0$, $B^{(l)}$, $l = 0, \dots, L$ are constants. We point out that $\sigma(\cdot)$ is a ReLU or a sigmoid function.

Analysing the Rademacher complexity allows up to obtain a data dependent bounds for our proposed model. Theorem 1 gives the Rademacher complexity for the AdaGPR.

Theorem 1. *Given the hypothesis class \mathcal{F} , the Rademacher complexity of the AdaGPR is bounded by*

$$\begin{aligned} Q^{-1} \mathcal{R}(\mathcal{F}, p) \leq C' \alpha & \left[2\sqrt{p} B^{(0)} \sum_{l=1}^L (1 - \alpha)^l 2^l \prod_{j=0}^{l-1} B^{(L-j)} \left(\sum_{i=1}^N \sum_{k=0}^{K-1} \mu_k^{(L-j)} |\lambda_i|^k \right) \|X\|_F \right. \\ & \left. + \left(\sum_{l=1}^{L-1} (1 - \alpha)^l 2^l \prod_{j=0}^{l-1} B^{(L-1-j)} \left(\sum_{i=1}^N \sum_{k=0}^{K-1} \mu_k^{(L-1-j)} |\lambda_i|^k \right) + 1 \right) D \right]. \end{aligned} \quad (11)$$

where λ_t is the t th eigenvalues values of \tilde{A} , and D , and C' are constants.

We can extend the hypothesis class (10) to derive the hypothesis class for GCNII by setting $\mu_1^{(l)} = 1.0$, $l = 1, \dots, L$ and obtain the Rademacher complexity for GCNII. Then the following Corollary gives the Rademacher complexity of the GCNII.

Corollary 1. *The Rademacher complexity of the GCNII is bounded as*

$$\begin{aligned} Q^{-1} \mathcal{R}(\mathcal{F}, p) \leq C' \alpha & \left[\sqrt{2p} B^{(0)} \sum_{l=1}^L 2^l (1 - \alpha)^l \prod_{j=0}^{l-1} B^{(L-j)} \left(\sum_{i=1}^N |\lambda_i| \right) \|X\|_F \right. \\ & \left. + \left(\sum_{l=1}^{L-1} (1 - \alpha)^l 2^l \prod_{j=1}^{l-1} B^{(L-1-j)} \left(\sum_{i=1}^N |\lambda_i| \right) + 1 \right) D \right], \end{aligned} \quad (12)$$

where λ_t is the t th eigenvalues values of \tilde{A} , and D , and C' are constants.

Summations of powers of eigenvalue spectrum in (11) and (12) help us to understand the information mixing occurring at each layers. The use of the normalized adjacency matrix results in a eigenvalue spectrum of $1 = \lambda_1 \geq \lambda_2 \geq \dots \geq \lambda_N \geq -1$ and as k increases the summation of the eigenvalue spectrum with the higher powers shrink quickly. However, with a large k , the Rademacher complexity may become small but its model could be too small due to the oversmoothing effect induced by multiple applications of node aggregations which results in larger bias. The training error for a model with large bias cannot be minimized. Hence, a smaller k avoids oversmoothing and results in better generalization. It is also important to notice that the deeper layers have a strong influence

Properties	Cora	Citeseer	Chameleon	Cornell	Texas	Wisconsin
Classes	7	4	4	5	5	5
Nodes	2708	3327	2277	183	183	251
Edges	5429	4732	36101	295	309	499
Features	1433	3703	2325	1703	1703	1703

Table 1: Properties of datasets used for node-classification

on the overall generalization bound due to recursive summations. This indicates that the recursive multiplications of the spectral components of deeper layers and a large make the overall bias further large. Hence, in order have less oversmoothing at deeper layers and to have a small overall bias less convolution is preferred at deeper layers. This observation agrees with the experimental results (Table 4).

5 Experiments

In this section we discuss node classification experiments that we carried out to evaluate AdaGPR. Additionally, we discuss the behaviour of layer-wise sparse solutions of generalised Pagerank coefficients to understand the adaptive behaviour of AdaGPR.

5.1 Setup

We performed semi-supervised and fully-supervised node classification. Datasets and their properties used in our experiments are listed in Table 1. Since our method stems from GCNII, we used a similar experimental setting as in [3] and borrowed their reported results for baseline methods. In addition to the hyperparameters α_l , λ_l , weight decays, and dropout rates common with GCNII, the number of GPR coefficients K and in some cases (semi-supervised learning) weight decay for learning weights $v^{(l)}$ for GPR coefficients in (7) are considered as hyperparameters. We tuned hyperparameters based on the loss over the validation sets. The optimization method for all experiments is Adam with learning rate of 0.01. We use the publicly available processed data provided by [3]. Further, we use code from [3] to assist our implementations. The data and Pytorch based implementation of AdaGPR is available at <https://github.com/kishanwn/AdaGPR>. We carried out experiments on NVidia V100-PCIE-16GB GPUs hosted on Intel Xeon Gold 6136 processor servers.

5.2 Semi-Supervised Node Classification

We used the commonly used citation datasets Cora and Citeseer to evaluate performance of semi-supervised node classification. These datasets are split based on the commonly used setting [19] that results in training sets with 20 nodes per each class, test sets with 500 nodes, and validation sets with 1000 nodes. The number of coefficients of the GPR is considered a hyperparameter and selected from $(2, 3, 4, 8, 16)$. We used the same hyperparameter ranges as in [3] for λ , and dropout rates from $(0.1, \dots, 0.9)$. We fixed $\alpha = 0.1$ following [3]. We used separate weight decay rates for different learning weights in AdaGPR; $WD_1 \in (1.0, 0.1, 0.01)$ for $W^{(0)}$, $WD_2 = 0.0001$ for $W^{(l)}$, $l = 1, \dots, L$, and $WD_3 \in (1.0, 0.1, 0.01)$ for $v^{(l)}$ $l = 1, \dots, L$. WD_1 and WD_3 are selected from hyperparameter tuning (see Table 6 in Section B in the supplementary section). We borrowed results for baseline methods Vanilla GCN [6], JKNet [18], IncepGCN [16], and GCNII [3] from [3].

The Table 2 shows that classification accuracies for Cora using AdaGPR did not out-perform the accuracy produced by GCNII. However, AdaGPR has produced better performances for shallow networks with layers ranging from 2 to 16 compared to GCNII. AdaGPR achieved a slightly improved accuracy for Citeseer compared to GCNII. The noteworthy observation is that AdaGPR provides the best accuracy of 73.5 with 16 layers and 32 hidden units compared to the GCNII which used 32 layers and 256 hidden units. The stable accuracies with the increase in depth for both datasets shows robustness against oversmoothing of AdaGPR.

Dataset	Method	Layers					
		2	4	8	16	32	64
Cora	GCN	81.1	80.4	69.5	64.9	60.3	28.7
	GCN(Drop)	82.8	82.0	75.8	75.7	62.5	49.5
	JKNet	-	80.2	80.7	80.2	81.1	71.5
	JKNet(Drop)	-	83.3	82.6	83.0	82.5	83.2
	Incep	-	77.6	76.5	81.7	81.7	80.0
	Incep(Drop)	-	82.9	82.5	83.1	83.1	83.5
	GCNII (hidden 64)	82.2	82.6	84.2	84.6	85.4	85.5
	GCNII* (hidden 64)	80.2	82.3	82.8	83.5	84.9	85.3
	AdaGPR (hidden 32, GPR coeffs. 4)	83.8	84.5	84.8	85.0	85.0	85.0
Citeseer	GCN	70.8	67.7	30.2	18.3	25.0	20.0
	GCN(Drop)	72.3	70.6	61.4	57.2	41.6	34.4
	JKNet	-	68.7	67.7	69.8	68.2	63.4
	JKNet(Drop)	-	72.6	71.8	72.6	70.8	72.2
	Incep	-	69.3	68.4	70.2	72.6	71.0
	Incep(Drop)	-	72.7	71.4	72.5	72.6	71.0
	GCNII (hidden 256)	68.2	68.9	70.6	72.9	73.4	73.4
	GCNII* (hidden 256)	66.1	67.9	70.6	72.0	73.2	73.1
	AdaGPR (hidden 64, GPR coeffs. 16)	59.9	68.6	73.2	73.5	73.4	73.1

Table 2: Accuracy for semi-supervised node classification

5.3 Fully-Supervised Node Classification

We experimented with fully-supervised node classification using the standards baseline graph datasets of Cora, Citeseer, Chameleon, Cornell, Texas, and Wisconsin. As suggested in [15], all these datasets were randomly split into training, validation and testing sets consisting of nodes by each class with percentages of 60%, 20%, and 20%, respectively. We ran experiments over 10 different random splits as used in [3]. For fair comparisons with [3] we used the 64 hidden units for all methods. Hyperparameter sets for dropout rates, and K are same as fully-supervised learning. Similar to [3], we used a single weight decay selected from the set $(0.001, 0.0005, \dots, 1e-6)$, $\alpha \in (0.1, \dots, 0.9)$, and $\lambda \in (0.5, 1.0, 1.5)$.

The mean accuracy for node classification of AdaGPR and baseline methods (borrowed from [3]) are shown in the Table 3. These baseline methods are Vanilla GCN [6], GAT [?], Geom-GCN [15], APPNP [7], JKNet [18], IncepGCN [16], and GCNII [3]. We also experimented with GPR-GNN whose results are included in Table 3. In addition to accuracy of AdaGPR, we show the number of layers and number of GPR coefficients (K) in brackets that were selected from the hyperparameter tuning.

Form Table 3 we can see that AdaGPR has obtained comparable accuracies compared to GCNII for both Cora and Citeseer. For both these datasets the AdaGPR model required 64 layers similar to GCNII, hence, no scale down in the network size for AdaGPR. On the other hand Chameleon dataset has similar number of nodes as with Cora and Citeseer (Table 1), however, it has larger number of edges compared to Cora and Citeseer. This indicates that Chameleon has a highly dense adjacency matrix compared to Cora and Citeseer. Further, Chameleon indicates a fast decaying eigenvalue spectrum for its normalized adjacency matrix. This observation is reflected in AdaGPR model with 2 layers and 3 coefficients giving the best accuracy for Chameleon. Notice that GCNII also have used a smaller network (8 layers) for Chemeleon compared to other datasets. Further, it is noteworthy that GPR-GNN which is another shallow model has gained a accuracy comparable to AdaGPR for Chemeleon.

There is a significant high accuracy for the three small scale datasets of Cornell, Texas, and Wisconsin with AdaGPR compared to all the baseline methods. Again, we can see that the increased performance with AdaGPR are achieved for Cornell and Texas with less number of convolution layers compared to GCNII. These observations provide evidence that adaptive GPR can perform model compression while enhancing prediction accuracy.

Method	Dataset					
	Cora	Citeseer	Chameleon	Cornell	Texas	Wisconsin
GCN	85.77	73.68	28.18	52.70	52.16	45.88
GAT	86.37	74.32	42.93	54.32	58.38	49.41
Geom-GCN-I	85.19	77.99	60.31	56.76	57.58	58.24
Geom-GCN-P	84.93	75.14	60.90	60.81	67.57	64.12
Geom-GCN-S	85.27	74.71	59.96	55.68	59.73	56.67
APPNP	87.87	76.53	54.3	73.51	65.41	69.02
JKNet	85.25 (16)	75.85 (8)	60.07 (64)	57.30 (4)	56.49 (32)	48.82 (8)
JKNet(Drop)	87.46 (16)	75.96 (8)	62.08 (64)	61.08 (4)	57.30 (32)	50.59 (8)
Incep(Drop)	86.86 (8)	76.83 (8)	61.71 (4)	61.62 (16)	57.84 (8)	50.20 (8)
GPR-GNN	88.16	77.39	63.22	78.37	77.30	81.57
GCNII	88.49 (64)	77.08 (64)	60.61 (8)	74.86 (16)	69.46 (32)	74.12 (16)
GCNII*	88.01 (64)	77.13 (64)	62.48 (8)	76.49 (16)	77.84 (32)	81.57 (16)
AdaGPR	88.19 (64,3)	77.25 (64,4)	64.71 (2,3)	82.70 (4,2)	81.08 (4,4)	83.53 (16,3)

Table 3: Accuracy for fully-supervised node classification

5.4 Layer-wise GPR Adaptation

One of the main objectives to propose the AdaGPR is to achieve layer-wise adaptive convolution. We can quantitatively understand the amount of convolution by different orders of the normalized adjacency matrix at each layer by analysing the coefficients of the layer-wise generalized Pageranks. Due to the use of Sprasemax activation method we are able to achieve sparse coefficients helping us to interpret trained models. Next, we discuss a few examples of AdaGPR models (due to space limitation we only consider four datasets, however, we found similar behaviours for other datasets).

Tables 4 shows coefficients of a semi-supervised learning model for Cora with 8 layers and 4 Pagerank coefficients. Though there are no sparseness among coefficients, notice that there is a gradual change of coefficients from shallow layers to deep layers. As the layers increase from the first to the seventh layers the largest coefficient shift within the first two coefficients, while the forth coefficient becomes small. Recall that the coefficient at 0 represent the identity matrix with no graph convolution, hence, indicates that each layer need not have graph convolution. Furthermore, the final layer has a different structure compared the rest of the shallow layers indicating that higher order convolutions are more important at the deepest layer. We observed a different layer-wise adaptation for semi-supervised learning with Citeseer, which we discuss in the Section C of the supplementary section.

Table 4 further shows learned Pagerank coefficients of trained models for Chameleon, Cornell, and Texas datasets with fully-supervised node-classification. The trained model for Chameleon has graph convolution only at the second layer using the normalized adjacency matrix and the first layer act as a residual layer. The learned model for Cornell shows that only the first two layers apply graph convolutions with gradual adaptations of the GPR from shallow layers to deeper layers. An interesting observation is seen with the trained model for the Texas dataset, where it has no graph convolution in all four layers. By looking at these sparse GPR coefficients one may draw a conclusion that many of the above models (e.g. Texas) do not need any graph convolution at all. We have found that graph convolutions with higher orders are important during the learning process though the final trained model may have zeros or low values for their coefficients. For more details on coefficient evolution during the training for Texas refer to section C in the supplementary section.

6 Related Methods

Our proposed method is modelled as an extension of GCNII by learning generalized Pageranks at each layer. The proposed AdaGPR has a similar deep structure as GCNII with the addition of layer-wise generalized Pagerank convolutions. The most closely related model that enables adaptive learning as our proposed method is GPR-GNN [4]. As we explained in Section 2 GPR-GNN only has a single adaptive convolution layer compared to the deep network structure of AdaGPR. Similarly, PPNP and APPNP [7] apply a single Pagerank convolution in shallow models without layer-wise adaptiveness.

Layers	GPR Coeff.			
	0	1	2	3
1	0.2664	0.2606	0.2449	0.2279
2	0.2755	0.2601	0.2435	0.2207
3	0.2626	0.2733	0.2438	0.2201
4	0.2863	0.2574	0.2467	0.2093
5	0.2412	0.2861	0.2537	0.2188
6	0.2588	0.2726	0.2574	0.2111
7	0.2664	0.2854	0.2463	0.2017
8	0.1407	0.2933	0.2919	0.2740

(a) Cora (semi-supervised)

Layers	GPR Coeff.		
	0	1	2
1	1	0	0
2	0	1	0

(b) Chameleon

Layers	GPR Coeff.			
	0	1	2	3
1	1	0	0	0
2	1	0	0	0
3	1	0	0	0
4	1	0	0	0

(d) Texas

Table 4: Pagerank coefficients of learned models for Cora (semi-supervised), Cornell, Chamleon, and Texas.

Convolutions by high-order adjacency matrices have been employed in several GCN models. Mix-Hop [1] applies learning using higher order adjacency matrices for convolution at different hops from a node. ScatterGCN [12] is another method that uses higher orders of the adjacency matrix to use neighbourhoods from different steps. Both MixHop and ScatterGCN do not have multi-layer convolutions or adaptive learning. Hence, these methods are not designed to overcome oversmoothing or obtain interpretable models.

7 Limitations of the Work

The increased number of hyperparameters can be a practical limitation of AdaGPR, which need to be further investigated in the future.

8 Conclusions and Future Work

We proposed the AdaGPR to perform layer-wise adaptive graph convolution using generalized Pageranks within GCNII models. We provide generalization bounds to analyse the relationship between eigenvalue spectrum of a graph and the depth of the network and its effect on oversmoothing. We evaluate our proposed method using benchmark node-classification datasets to show performance improvements compared to other GCN models. By analysing coefficients of the generalized Pagerank in the trained models, we confirm that adaptive behaviour of graph convolution in each layer. Further, we demonstrate that our analysis of learned coefficients of generalized Pageranks helps us in interpreting layer-wise convolutions for different data and learning tasks.

We believe that our research opens up important directions for future research on adaptive graph convolution networks. One of the interesting research direction is to investigate adaptive generalized Pageranks more broadly with graph neural networks such as message passing methods and attention networks. The ability to obtain sparse solutions for the generalized Pagerank is a motivation for further investigations towards model compression and neural architecture search for GCN models. Furthermore, investigation into novel neural architecture search methods could also be conducive to overcome the limitation of large number of hyperparameter tuning associated with AdaGPR. Further theoretical analysis on generalization bounds using Pac-Bayes analysis [10] AdaGPR could provide further understanding on adaptive GCN models and Pagerank based convolutions.

References

- [1] ABU-EL-HAIJA, S., PEROZZI, B., KAPOOR, A., ALIPOURFARD, N., LERMAN, K., HARUTYUNYAN, H., STEEG, G. V., AND GALSTYAN, A. MixHop: Higher-order graph convolutional architectures via sparsified neighborhood mixing. In *ICML* (2019).
- [2] BRIN, S., AND PAGE, L. The anatomy of a large-scale hypertextual web search engine. *Computer Networks and ISDN Systems* 30, 1 (1998), 107–117. Proceedings of the Seventh International World Wide Web Conference.
- [3] CHEN, M., WEI, Z., HUANG, Z., DING, B., AND LI, Y. Simple and deep graph convolutional networks. In *ICML* (13–18 Jul 2020), vol. 119, PMLR, pp. 1725–1735.
- [4] CHIEN, E., PENG, J., LI, P., AND MILENKOVIC, O. Adaptive universal generalized pagerank graph neural network. In *ICML* (2021).
- [5] EL-YANIV, R., AND PECHYONY, D. Transductive rademacher complexity and its applications. *J. Artif. Int. Res.* 35, 1 (2009).
- [6] KIPF, T. N., AND WELLING, M. Semi-Supervised Classification with Graph Convolutional Networks. In *ICLR* (2017), ICLR '17.
- [7] KLICPERA, J., BOJCHEVSKI, A., AND GÜNNEMANN, S. Predict then propagate: Graph neural networks meet personalized pagerank. In *ICLR 2019* (2019).
- [8] LI, C., AND GOLDWASSER, D. Encoding social information with graph convolutional networks for Political perspective detection in news media. In *Proceedings of the 57th Annual Meeting of the Association for Computational Linguistics* (Florence, Italy, July 2019), pp. 2594–2604.
- [9] LI, P., CHIEN, E., AND MILENKOVIC, O. Optimizing generalized pagerank methods for seed-expansion community detection. *NeurIPS* 32 (2019).
- [10] LIAO, R., URTASUN, R., AND ZEMEL, R. S. A pac-bayesian approach to generalization bounds for graph neural networks. In *NeurIPS* (2020).
- [11] MARTINS, A. F. T., AND ASTUDILLO, R. F. From softmax to sparsemax: A sparse model of attention and multi-label classification. In *ICML* (2016), JMLR.org.
- [12] MIN, Y., WENKEL, F., AND WOLF, G. Scattering GCN: overcoming oversmoothness in graph convolutional networks. *CoRR abs/2003.08414* (2020).
- [13] OONO, K., AND SUZUKI, T. Graph neural networks exponentially lose expressive power for node classification. In *ICLR 2020* (2020).
- [14] OONO, K., AND SUZUKI, T. Optimization and generalization analysis of transduction through gradient boosting and application to multi-scale graph neural networks. In *NeurIPS 2020* (2020).
- [15] PEI, H., WEI, B., CHANG, K. C., LEI, Y., AND YANG, B. Geom-gcn: Geometric graph convolutional networks. In *ICLR 2020* (2020), ICLR'20.
- [16] RONG, Y., HUANG, W., XU, T., AND HUANG, J. Dropedge: Towards deep graph convolutional networks on node classification. In *ICLR 2020* (2020).
- [17] SCHLICHTKRULL, M., KIPF, T. N., BLOEM, P., VAN DEN BERG, R., TITOV, I., AND WELLING, M. Modeling relational data with graph convolutional networks. In *The Semantic Web* (Cham, 2018), Springer International Publishing, pp. 593–607.
- [18] XU, K., LI, C., TIAN, Y., SONOBE, T., KAWARABAYASHI, K.-I., AND JEGETKA, S. Representation learning on graphs with jumping knowledge networks. In *ICML* (10–15 Jul 2018), vol. 80, pp. 5453–5462.
- [19] YANG, Z., COHEN, W. W., AND SALAKHUTDINOV, R. Revisiting semi-supervised learning with graph embeddings. *ICML'16*, p. 40–48.
- [20] YING, R., HE, R., CHEN, K., EKSOMBATCHAI, P., HAMILTON, W. L., AND LESKOVEC, J. Graph convolutional neural networks for web-scale recommender systems. In *KDD '18* (2018).
- [21] ZHAO, L., AND AKOGLU, L. Pairnorm: Tackling oversmoothing in gnns. In *ICLR 2020* (2020).
- [22] ZHAO, L., PENG, X., TIAN, Y., KAPADIA, M., AND METAXAS, D. N. Semantic graph convolutional networks for 3d human pose regression. In *(CVPR)* (2019), pp. 3425–3435.

Supplementary Material Section

A Proofs of Generalization Bounds

In this section we provide detailed proofs of Theorems given in the Section 4.

The following transductive Rademacher complexity is defined in [5].

Definition 1. *Given $p \in [0, 0.5]$ and $\mathcal{V} \subset \mathbb{R}^N$, the transductive Rademacher complexity is defined as*

$$\mathcal{R}(\mathcal{V}, p) = Q \mathbb{E}_\epsilon \left[\sup_{v \in \mathcal{V}} \langle \epsilon, v \rangle \right],$$

where $Q = \frac{1}{M} + \frac{1}{N}$ and $\epsilon = (\epsilon_1, \dots, \epsilon_N)$ is a sequence of i.i.d. Rademacher variables with distribution $\mathbb{P}(\epsilon_i = 1) = \mathbb{P}(\epsilon_i = -1) = p$ and $\mathbb{P}(\epsilon_i = 0) = 1 - 2p$. We denote $\mathcal{R}(\mathcal{V}) := \mathcal{R}(\mathcal{V}, p_0)$ when $p_0 = \frac{MU}{(M+U)^2}$.

Below we restate the symmetric Rademacher complexity [14], a variant of the above transductive Rademacher complexity.

Definition 2. *Given $p \in [0, 0.5]$ and $\mathcal{V} \subset \mathbb{R}^N$, the symmetric transductive Rademacher complexity is defined as*

$$\bar{\mathcal{R}}(\mathcal{V}, p) = Q \mathbb{E}_\epsilon \left[\sup_{v \in \mathcal{V}} \langle \epsilon, v \rangle \right],$$

where $Q = \frac{1}{M} + \frac{1}{N}$ and $\epsilon = (\epsilon_1, \dots, \epsilon_N)$ is a sequence of i.i.d. Rademacher variables with distribution $\mathbb{P}(\epsilon_i = 1) = \mathbb{P}(\epsilon_i = -1) = p$ and $\mathbb{P}(\epsilon_i = 0) = 1 - 2p$. We denote $\bar{\mathcal{R}}(\mathcal{V}) := \bar{\mathcal{R}}(\mathcal{V}, p_0)$ when $p_0 = \frac{MU}{(M+U)^2}$.

In [14], it has been shown that $\mathcal{R}(\mathcal{V}, p) \leq \bar{\mathcal{R}}(\mathcal{V}, p)$.

Below we provide the proof for the Theorem 1.

Proof of Theorem 1. We use the symmetric Rademacher complexity

$$\mathcal{R}(\mathcal{F}, p) = \mathbb{E}_\epsilon \left[\sup_{v \in \mathcal{F}} |\langle \epsilon, v \rangle| \right], \quad (13)$$

which upper bounds the Rademacher complexity $\mathcal{R}(\mathcal{F})$ in (9).

In the rest of the proof we abbreviate row s of any matrix Z by $Z_s := Z[s, :]$, columns c by $Z_{\cdot c} := Z[:, c]$, and an element by $Z_{sc} := Z[s, c]$. For the convenience of analysis we break the hypothesis class \mathcal{F} in (10) into different components and define

$$\begin{aligned} \mathcal{H}^{(0)} &= \left\{ \sum_{c=1}^{C_0} X_{\cdot c} w_c^{(0)} \mid \|w_c^{(0)}\|_1 \leq B^{(0)} \right\}, \\ \tilde{\mathcal{H}}^{(0)} &= \sigma \circ \mathcal{H}^{(0)}, \\ \mathcal{H}^{(l+1)} &= \left\{ \sum_{c=1}^{C_{l+1}} ((1-\alpha)[\tilde{A}(\mu)Z]_{\cdot c} + \alpha H_{\cdot c}) w_c^{(l)} \mid Z_{\cdot c} \in \tilde{\mathcal{H}}^{(l)}, H_{\cdot c} \in \tilde{\mathcal{H}}^{(0)}, \|w_c^{(l)}\|_1 \leq B^{(l)} \right\}, \\ \mathcal{G}^{(l+1)} &= \left\{ \sum_{k=0}^{K-1} \mu_k^{(l+1)} \tilde{A}^k \mid \sum_{k=0}^{K-1} \mu_k^{(l+1)} = 1, \|\tilde{A}\|_1 \leq \sqrt{d} \right\}, \\ \tilde{\mathcal{H}}^{(l+1)} &= \sigma \circ \mathcal{H}^{(l)} \quad l = 1, \dots, L. \end{aligned}$$

Now, for a given layer $l + 1$, we have

$$\begin{aligned}
Q^{-1}\mathcal{R}(\tilde{\mathcal{H}}^{(l+1)}, p) &= \mathbb{E}_\epsilon \left[\sup_{\|w^{(l)}\|_1 \leq B^{(l)}, Z_{\cdot c} \in \mathcal{H}^{(l)}, H_{\cdot c} \in \tilde{\mathcal{H}}^{(0)}, \tilde{A}(\mu^{(l)}) \in \mathcal{G}} \left| \sum_{n=1}^N \epsilon_n \sum_{c=1}^{C_{l+1}} ((1-\alpha)[\tilde{A}(\mu^{(l)})Z]_{nc} + \alpha H_{nc}) w_c^{(l)} \right| \right] \\
&= \mathbb{E}_\epsilon \left[\sup_{\|w^{(l)}\|_1 \leq B^{(l)}, Z_{\cdot c} \in \mathcal{H}^{(l)}, H_{\cdot c} \in \tilde{\mathcal{H}}^{(0)}, \tilde{A}(\mu^{(l)}) \in \mathcal{G}} \left| \sum_{c=1}^{C_{l+1}} \sum_{n=1}^N \epsilon_n ((1-\alpha)[A(\mu^{(l)})Z]_{nc} + \alpha H_{nc}) w_c^{(l)} \right| \right] \\
&= B^{(l)} \mathbb{E}_\epsilon \left[\sup_{Z \in \mathcal{H}^{(l)}, H \in \tilde{\mathcal{H}}^{(0)}, \tilde{A}(\mu^{(l)}) \in \mathcal{G}} \left| \sum_{n=1}^N \epsilon_n ((1-\alpha)[\tilde{A}(\mu^{(l)})Z]_n + \alpha H_n) \right| \right] \\
&= B^{(l)} \mathbb{E}_\epsilon \left[\sup_{Z \in \mathcal{H}^{(l)}, H \in \tilde{\mathcal{H}}^{(0)}, \tilde{A}(\mu^{(l)}) \in \mathcal{G}} \left| (1-\alpha) \sum_{n=1}^N \epsilon_n [\tilde{A}(\mu^{(l)})Z]_n + \alpha \sum_{n=1}^N \sigma_n H_n \right| \right] \\
&= B^{(l)} (1-\alpha) \mathbb{E}_\epsilon \left[\sup_{Z \in \mathcal{H}^{(l)}, \tilde{A}(\mu^{(l)}) \in \mathcal{G}} \left| \sum_{n=1}^N \epsilon_n [\tilde{A}(\mu^{(l)})Z]_n \right| \right] \\
&\quad + \alpha B^{(l)} \mathbb{E}_\epsilon \left[\sup_{H \in \tilde{\mathcal{H}}^{(0)}} \left| \sum_{n=1}^N \epsilon_n H_n \right| \right]. \tag{14}
\end{aligned}$$

We have,

$$\begin{aligned}
\mathbb{E}_\epsilon \left[\sup_{Z \in \mathcal{H}^{(l)}} \left| \sum_{n=1}^N \epsilon_n [\tilde{A}(\mu^{(l)})Z]_n \right| \right] &= \mathbb{E}_\epsilon \left[\sup_{Z \in \mathcal{H}^{(l)}} \left| \sum_{n=1}^N \epsilon_n [\tilde{A}(\mu^{(l)})\mathbb{E}_{\epsilon'}[\epsilon' \epsilon'^\top]Z]_n \right| \right] \quad (\because \mathbb{E}_{\epsilon'}[\epsilon' \epsilon'^\top] = I) \\
&\leq \mathbb{E}_{\epsilon, \epsilon'} \left[\sup_{Z \in \mathcal{H}^{(l)}} \left| \epsilon^\top \tilde{A}(\mu^{(l)})\epsilon' \epsilon'^\top Z \right| \right] \leq \mathbb{E}_{\epsilon, \epsilon'} \left[\left| \epsilon^\top \tilde{A}(\mu^{(l)})\epsilon' \right| \sup_{Z \in \mathcal{H}^{(l)}} |\epsilon'^\top Z| \right] \\
&= \mathbb{E}_{\epsilon'} \left[\mathbb{E}_\epsilon \left[\left| \epsilon^\top \tilde{A}(\mu^{(l)})\epsilon' \right| \right] \sup_{Z \in \mathcal{H}^{(l)}} |\epsilon'^\top Z| \right] \\
&\leq \mathbb{E}_{\epsilon'} \left[\sqrt{\mathbb{E}_\epsilon \left[\left(\epsilon^\top \tilde{A}(\mu^{(l)})\epsilon' \right)^2 \right]} \sup_{Z \in \mathcal{H}^{(l)}} |\epsilon'^\top Z| \right] = \mathbb{E}_{\epsilon'} \left[\sqrt{\mathbb{E}_\epsilon \left[\epsilon'^\top \tilde{A}(\mu^{(l)})\epsilon \epsilon^\top \tilde{A}(\mu^{(l)})\epsilon' \right]} \sup_{Z \in \mathcal{H}^{(l)}} |\epsilon'^\top Z| \right] \\
&= \mathbb{E}_{\epsilon'} \left[\sqrt{\epsilon'^\top \tilde{A}(\mu^{(l)})^2 \epsilon'} \sup_{Z \in \mathcal{H}^{(l)}} |\epsilon'^\top Z| \right].
\end{aligned}$$

Here, by the Hanson-Wright concentration inequality implies that

$$\mathbb{P}[\epsilon'^\top \tilde{A}(\mu^{(l)})\epsilon' - \mathbb{E}_{\epsilon'}[\epsilon'^\top \tilde{A}(\mu^{(l)})\epsilon']] \geq c(\|\tilde{A}(\mu^{(l)})\|_F \sqrt{t} + \|\tilde{A}(\mu^{(l)})\|t) \leq \exp(-t) \quad (t > 0),$$

with a universal constant c , where $\|A\|_F = \sqrt{\text{Tr}[AA^\top]}^2$. Moreover, Talagrand's concentration inequality yields

$$\mathbb{P} \left[\left| \sup_{Z \in \mathcal{H}^{(l)}} \epsilon'^\top Z \right| \geq c' \left(\mathbb{E}_{\epsilon'} \left[\left| \sup_{Z \in \mathcal{H}^{(l)}} \epsilon'^\top Z \right| \right] + \sqrt{Nt \sup_{Z \in \mathcal{H}^{(l)}} \sum_{n=1}^N Z_n^2/N + t \sup_{Z \in \mathcal{H}^{(l)}} \|Z\|_\infty} \right) \right] \leq e^{-t} \quad (t > 0),$$

where $c' > 0$ is a universal constant. Then, by noticing that $\mathbb{E}_{\epsilon'}[\epsilon'^\top A \epsilon'] = \text{Tr}[A]$, these inequalities yield

$$\begin{aligned}
&\mathbb{E}_{\epsilon'} \left[\sqrt{\epsilon'^\top \tilde{A}(\mu^{(l)})^2 \epsilon'} \sup_{Z \in \mathcal{H}^{(l)}} |\epsilon'^\top Z| \right] \\
&\leq \int \sqrt{\text{Tr}[\tilde{A}(\mu^{(l)})^2] + c(\|\tilde{A}(\mu^{(l)})^2\|_F \sqrt{t} + \|\tilde{A}(\mu^{(l)})^2\|t)} \\
&\quad c'(|\mathbb{E}_{\epsilon'} \sup_{Z \in \mathcal{H}^{(l)}} \epsilon'^\top Z| + \sqrt{t} \|\mathcal{H}^{(l)}\|_2 + t \|\mathcal{H}^{(l)}\|_\infty) 2 \exp(-t) dt
\end{aligned}$$

²There also exists a uniform type Hanson-Wright inequality.

where we define $\|\mathcal{H}^{(l)}\|_k := \sup_{Z \in \mathcal{H}^{(l)}} \|Z\|_k$. The right hand side can be further bounded as $C\sqrt{\text{Tr}[\tilde{A}(\mu^{(l)})^2]} (\mathbb{E}_{\epsilon'} [\sup_{Z \in \mathcal{H}^{(l)}} \epsilon'^\top Z] + \|\mathcal{H}^{(l)}\|_2)$ for a universal constant C .

Since the output is bounded we can assume that $\sup_{Z \in \mathcal{H}^{(l)}} \|Z\|_2 \leq D$ where D is a data dependent constant. Now substituting the above result back to (14), we have

$$\begin{aligned}
Q^{-1}\mathcal{R}(\tilde{\mathcal{H}}^{(l+1)}, p) &\leq B^{(l)}(1-\alpha) \left[C\sqrt{\text{Tr}[\tilde{A}(\mu^{(l)})^2]} \mathbb{E}_{\epsilon} \left| \sup_{Z \in \mathcal{H}^{(l)}} \left(\sum_{n=1}^N \epsilon_n Z_n \right) \right| + D \right] \\
&\quad + \alpha B^{(l)} \mathbb{E}_{\epsilon} \left[\sup_{H \in \tilde{\mathcal{H}}^{(0)}} \left| \sum_{n=1}^N \epsilon_n H_n \right| \right] \\
&\leq B^{(l)}(1-\alpha) \left[C \sqrt{\sum_{i=1}^N \left(\sum_{k=0}^{K-1} \mu_k^{(l)} \lambda_i^k \right)^2} \mathbb{E}_{\epsilon} \sup_{Z \in \mathcal{H}^{(l)}} \left| \left(\sum_{n=1}^N \epsilon_n Z_n \right) \right| + D \right] \\
&\quad + \alpha B^{(l)} \mathbb{E}_{\epsilon} \left[\sup_{H \in \tilde{\mathcal{H}}^{(0)}} \left| \sum_{n=1}^N \epsilon_n H_n \right| \right] \\
&= CB^{(l)}(1-\alpha) \left[\left(\sum_{i=1}^N \sum_{k=0}^{K-1} \mu_k^{(l)} |\lambda_i|^k \right) Q^{-1}\mathcal{R}(\mathcal{H}^{(l)}, p) + D \right] \\
&\quad + \alpha B^{(l)} \mathbb{E}_{\epsilon} \left[\sup_{H \in \tilde{\mathcal{H}}^{(0)}} \left| \sum_{n=1}^N \epsilon_n H_n \right| \right], \tag{15}
\end{aligned}$$

where λ_t is the t -th eigenvalue of \tilde{A} and we have used the used $\sqrt{\sum_{i=1}^N (\sum_{k=0}^{K-1} \mu_k^{(l)} \lambda_i^k)^2} \leq \sum_{i=1}^N \sqrt{(\sum_{k=0}^{K-1} \mu_k^{(l)} \lambda_i^k)^2} = \sum_{i=1}^N \left| \sum_{k=0}^{K-1} \mu_k^{(l)} \lambda_i^k \right| \leq \sum_{i=1}^N \sum_{k=0}^{K-1} \mu_k^{(l)} |\lambda_i|^k$.

Since σ is 1-Lipschitz using the contraction property from Proposition 10 of [14], we have

$$\mathcal{R}(\mathcal{H}^{l+1}, p) \leq 2\mathcal{R}(\tilde{\mathcal{H}}^{l+1}, p),$$

leading to reduction in (15) to

$$\begin{aligned}
Q^{-1}\mathcal{R}(\tilde{\mathcal{H}}^{l+1}, p) &\leq C2^l B^{(l)}(1-\alpha) \left[\left(\sum_{i=1}^N \sum_{k=0}^{K-1} \mu_k^{(l)} |\lambda_i|^k \right) Q^{-1}\mathcal{R}_S(\tilde{\mathcal{H}}^l, p) + D \right] \\
&\quad + \alpha B^{(l)} \mathbb{E}_{\epsilon} \left[\sup_{H \in \tilde{\mathcal{H}}^{(0)}} \left| \sum_{n=1}^N \epsilon_n H_n \right| \right]. \tag{16}
\end{aligned}$$

Given that $\mathcal{F} = \tilde{\mathcal{H}}^{L+1}$, the final reduction using (16) leads to

$$\begin{aligned}
Q^{-1}\mathcal{R}(\mathcal{F}, p) &\leq C' \alpha \sum_{l=1}^L (1-\alpha)^l 2^l \prod_{j=0}^{l-1} B^{(L-j)} \left(\sum_{i=1}^N \sum_{k=0}^{K-1} \mu_k^{(L-j)} |\lambda_i|^k \right) \mathbb{E}_{\epsilon} \left[\sup_{H \in \tilde{\mathcal{H}}^{(0)}} \left| \sum_{n=1}^N \epsilon_n H_n \right| \right] \\
&\quad + C' \alpha \left(\sum_{l=1}^{L-1} (1-\alpha)^l 2^l \prod_{j=0}^{l-1} B^{(L-1-j)} \left(\sum_{i=1}^N \sum_{k=0}^{K-1} \mu_k^{(L-1-j)} |\lambda_i|^k \right) + 1 \right) D. \tag{17}
\end{aligned}$$

By construction of \mathcal{F} , we know that $\mathcal{R}(\mathcal{H}^0, p) = \mathbb{E}_\epsilon \left[\sup_{H \in \tilde{\mathcal{H}}^{(0)}} \left| \sum_{n=1}^N \epsilon_n H_n \right| \right]$, and following [14], we have

$$\begin{aligned}
\mathcal{R}(\mathcal{H}^{(0)}, p) &= \mathbb{E}_\epsilon \left[\max_{c \in [C]} \left| \sum_{n=1}^N \epsilon_n X_{nc} \right| \right] \\
&= \mathbb{E}_\epsilon \left[\max_{c \in [C]} \left| \left(\sum_{n=1}^N \epsilon_n X_n \right) W_{\cdot c}^{(0)} \right| \right] \\
&\leq \mathbb{E}_\epsilon \left[\max_{c \in [C]} \|W_{\cdot c}^{(0)}\|_2 \left\| \sum_{n=1}^N \epsilon_n X_n \right\|_2 \right] \\
&\leq B^{(0)} \mathbb{E}_\epsilon \left\| \sum_{n=1}^N \epsilon_n X_n \right\|_2 \\
&\leq B^{(0)} \sqrt{\mathbb{E}_\epsilon \sum_{c=1}^C \left(\sum_{n=1}^N \epsilon_n X_n \right)^2} \quad (\text{Jensen Inequality}) \\
&= B^{(0)} \sqrt{\mathbb{E}_\epsilon \sum_{c=1}^C \left(\sum_{n=1}^N \epsilon_n X_n \right)^2} \\
&= B^{(0)} \sqrt{\mathbb{E}_\epsilon \sum_{c=1}^C \sum_{n,m=1}^N \epsilon_n \epsilon_m X_{nc} X_{mc}} \\
&= B^{(0)} \sqrt{\sum_{c=1}^C \sum_{m=1}^N 2p(X_{mc})^2} \\
&= B^{(0)} \sqrt{2p} \|X\|_{\text{F}}.
\end{aligned} \tag{18}$$

By combining (18) with (17), the resulting final Rademacher complexity bound is given by

$$\begin{aligned}
Q^{-1} \mathcal{R}(\mathcal{F}, p) &\leq C' \alpha \left[2\sqrt{p} B^{(0)} \sum_{l=1}^L (1-\alpha)^l 2^l \prod_{j=0}^{l-1} B^{(L-j)} \left(\sum_{i=1}^N \sum_{k=0}^{K-1} \mu_k^{(L-j)} |\lambda_i|^k \right) \|X\|_{\text{F}} \right. \\
&\quad \left. + \left(\sum_{l=1}^{L-1} (1-\alpha)^l 2^l \prod_{j=0}^{l-1} B^{(L-1-j)} \left(\sum_{i=1}^N \sum_{k=0}^{K-1} \mu_k^{(L-1-j)} |\lambda_i|^k \right) + 1 \right) D \right]. \tag{19}
\end{aligned}$$

Proof of Corollary 1. To convert AdaGPR to GCNII we replace the generalized Pagerank $\tilde{A}(\mu)$ with the normalized adjacency matrix \tilde{A} , which is equivalent to setting $\mu_1^{(l)} = 1$ and rest of the elements in $\mu^{(l)}$ to zero. This reduces the (19) to

$$\begin{aligned}
Q^{-1} \mathcal{R}(\mathcal{F}, p) &\leq C' \sqrt{2p} B^{(0)} \alpha \sum_{l=1}^L 2^l (1-\alpha)^l \prod_{j=0}^{l-1} B^{(L-j)} \left(\sum_{i=1}^N |\lambda_i| \right) \|X\|_{\text{F}} \\
&\quad + C' \alpha \left(\sum_{l=1}^{L-1} (1-\alpha)^l 2^l \prod_{j=1}^{l-1} B^{(L-1-j)} \left(\sum_{i=1}^N |\lambda_i| \right) + 1 \right) D.
\end{aligned}$$

B Summary of Hyperparameter Selection

In this section we discuss provide the details of hyperparameter selected for the proposed method though the validation process.

Dataset	GPR Coeffs.	LR	WD ₁	WD ₂	WD ₃	λ	α	Dropout
Cora	4	0.01	1.0	0.0001	0.1	0.1	0.3	0.6
Citeseer	16	0.01	1.0	0.0001	0.1	0.5	0.1	0.1

Table 5: Hyperparameters for semi-supervised node-classification

Dataset	GPR Coeffs.	layers	LR	Weight Decay	λ	α	Dropout
Cora	3	64	0.01	0.0001	0.5	0.1	0.5
Citeseer	2	64	0.01	0.0001	0.5	0.4	0.7
Chameleon	3	2	0.01	0.001	1.5	0.6	0.6
Cornell	2	4	0.01	0.0001	1.0	0.9	0.4
Texas	4	4	0.01	5e-4	1.0	0.5	0.5
Wisconsin	3	16	0.01	5e-5	1.5	0.6	0.3

Table 6: Hyperparameters for fully-supervised node-classification

For both experiments, we tuned the number of coefficients of the GPR as a hyperparameter selection from the set of $\{2, 3, 4, 8, 16, 32\}$. For fully-supervised node-classification, we used the same parameter ranges as in GCNII [3]; 64 hidden units, learning rate 0.01, the number of layers from $\{2, 4, 8, 16, 32, 64\}$, $\lambda \in (0.5, 1.0, 1.5)$, $\alpha \in (0.1, 0.2, \dots, 0.9)$, dropout $\in (0.1, 0.2, \dots, 0.9)$, and weight decay $\in (0.001, 5e-3, \dots, 1e-6)$.

For semi-supervised node-classification, we fixed the learning rate with 0.01 and $\alpha = 0.1$ as given in [3]. We set the weight decay rate $L_2 = 0.0001$ and applied hyperparameter tuning for weight decays for L_1 and L_3 from the set $\{1.0, 0.1, 0.01\}$. Further we performed hyperparameter tuning for $\lambda \in (0.1, 0.2, \dots, 0.9)$, dropout $\in (0.1, 0.2, \dots, 0.9)$, and number of coefficients of the GPR K from the set $\{2, 3, 4, 8, 16\}$.

Details of the parameters selected using hyperparameter tuning for semi-supervised node classification and fully-supervised node-classification by the AdaGPR are listed in Tables 6 and 5, respectively.

C Further Analysis of Trained Models

Table 7 shows the GPR coefficients for semi-supervised node classification for Citeseer dataset using 16 layers and 16 GPR coefficients. Notice that coefficients in shallow layers, layer 1 to layer 8, roughly equal to 1/16. By analysing the learning parameters for coefficients, we found that this is due to small values of the learning parameters in shallow layers. This may have caused by the application of softmax-like (sparsemax) activation to a set of values that are close to zeros. As the layers increases beyond 8, coefficients start to deviate and it becomes clear that each layer applies convolution with a different generalized Pagerank. Furthermore, it is worth noticing that with the increase in layers the value of the first coefficient becomes prominent and the coefficients for the higher order terms gradually decreases.

In Figure 1 we show the change of values in GPR coefficients at each iteration with fully-supervised node classification for Texas dataset with a AdaGPR model that consist of 4 convolution layers and 4 GPR coefficients.

Layers	GPR Coeff.														
	0	1	2	3	4	5	6	7	8	9	10	11	12	13	14
1	0.063	0.063	0.063	0.063	0.063	0.063	0.063	0.062	0.062	0.062	0.062	0.062	0.062	0.062	0.062
2	0.063	0.063	0.063	0.063	0.063	0.063	0.063	0.062	0.062	0.062	0.062	0.062	0.062	0.062	0.062
3	0.063	0.063	0.063	0.063	0.063	0.063	0.063	0.062	0.062	0.062	0.062	0.062	0.062	0.062	0.062
4	0.063	0.063	0.063	0.063	0.063	0.063	0.063	0.062	0.062	0.062	0.062	0.062	0.062	0.062	0.062
5	0.064	0.064	0.063	0.063	0.063	0.063	0.063	0.063	0.062	0.062	0.062	0.062	0.062	0.062	0.061
6	0.064	0.064	0.064	0.064	0.063	0.063	0.063	0.062	0.062	0.062	0.062	0.062	0.061	0.062	0.061
7	0.065	0.065	0.064	0.064	0.064	0.063	0.063	0.063	0.062	0.062	0.062	0.061	0.061	0.061	0.060
8	0.066	0.066	0.066	0.065	0.064	0.064	0.063	0.063	0.062	0.062	0.061	0.060	0.060	0.060	0.059
9	0.068	0.069	0.067	0.066	0.065	0.064	0.063	0.063	0.062	0.061	0.061	0.060	0.059	0.059	0.058
10	0.072	0.070	0.069	0.067	0.065	0.065	0.064	0.063	0.062	0.061	0.060	0.058	0.058	0.057	0.056
11	0.077	0.075	0.072	0.069	0.070	0.067	0.064	0.062	0.060	0.059	0.057	0.056	0.055	0.054	0.052
12	0.090	0.084	0.078	0.074	0.071	0.067	0.064	0.061	0.059	0.056	0.054	0.052	0.050	0.048	0.046
13	0.135	0.102	0.091	0.080	0.074	0.068	0.062	0.057	0.055	0.049	0.045	0.042	0.040	0.036	0.033
14	0.280	0.132	0.107	0.085	0.072	0.061	0.052	0.044	0.038	0.032	0.027	0.022	0.018	0.014	0.011
15	0.557	0.147	0.109	0.069	0.050	0.032	0.021	0.010	0.001	0.001	0.002	0.001	0.000	0.000	0.000
16	0.879	0.080	0.039	0.002	0.000	0.000	0.000	0.000	0.000	0.000	0.000	0.000	0.000	0.000	0.000

Table 7: GPR coefficients of a trained AdaGPR model for Semi-supervised learning with Citeseer.

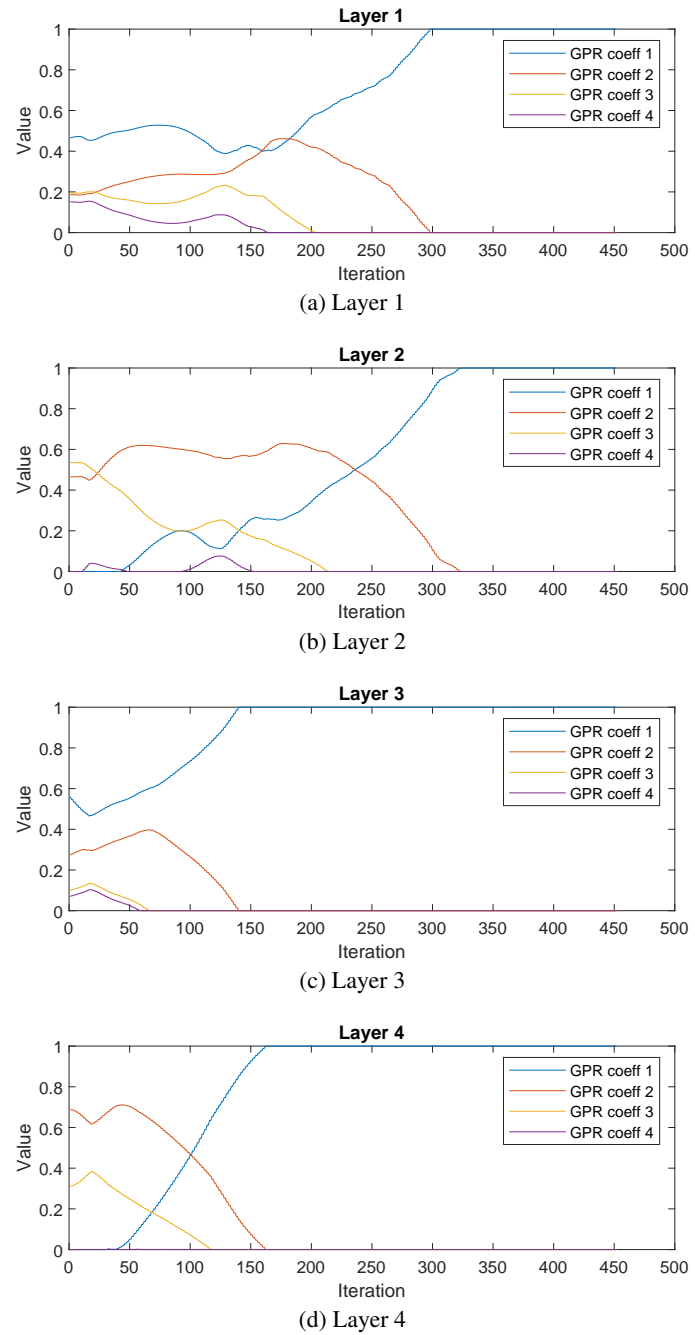


Figure 1: Change of GPR coefficients during optimization with Texas dataset for a model with 4 layers and 4 GPR coefficients